https://doi.org/10.33271/nvngu/2024-1/050

B. Eller[1,2],
orcid.org/0000-0001-7253-1757,
S. Szalai[1],
orcid.org/0000-0001-6440-1135,
M. Sysyn[3],
orcid.org/0000-0001-6893-0018,
D. Harrach[1],
orcid.org/0000-0003-4819-8506,
J. Liu[4],
orcid.org/0000-0002-4779-7761,
S. Fischer[*1],
orcid.org/0000-0001-7298-9960

1 – Szechenyi Istvan University, Gyor, Hungary
2 – University of Pecs, Pecs, Hungary
3 – Institute of Railway Systems and Public Transport, TU Dresden, Dresden, the Federal Republic of Germany
4 – China Railway First Group Xinyun Engineering Co., Ltd, Xi'an, the People's Republic of China
[*] Corresponding author e-mail: fischersz@sze.hu

ADVANTAGES OF USING CONCRETE CANVAS MATERIALS IN RAILWAY TRACK CONSTRUCTION

Purpose. Justification of the feasibility of using new types of drainage materials, such as Concrete Canvas (CC), under the upper structure of the railway permanent way.

Methodology. The tasks were solved by a complex research method, including analysis and generalization of literary and patent sources, analytical, experimental studies, using computer and mathematical modeling methods. Tests were conducted with and without the CC layer in a multi-level shear box. After the shear test, the specimens were also tested for load-bearing capacity (E_2, according to the Hungarian standard) and particle breakage. The contact surface between the bottom of the ballast and the CC was measured using a precision 3D laser scanner (GOM ATOS) and visualized graphically using AutoCAD software.

Findings. Experimental testing of the vertical load during connection and analysis compared with the test results of geocomposite/geogrid structures, internal shear resistance, and other parameters proved the structure's higher load-bearing capacity with the CC layer. Based on the results, the Concrete Canvas structure provides higher reinforcement than the average geogrid type.

Originality. The advantages of using new Concrete Canvas materials in the structure of a railway track have been demonstrated for the first time to provide greater internal shear resistance than the average for geogrids.

Practical value. These results may provide primary data for using Concrete Canvas in railway tracks and superstructures in the future.

Keywords: *railway,* Concrete Canvas*, ballasted track, inner shear resistance, geogrid, GOM ATOS*

Introduction. This article deals with some aspects of sustainability, mainly from the perspective of the field of transport infrastructure within civil engineering, i.e., geotechnical and railway engineering. When examined in isolation, this field is challenging to come by and typically transport(ation) sciences [1, 2], logistics [3–5], mining, geology, rock physics [6–8], architecture and civil engineering [9–11], mechanical and vehicle engineering [12,13], mechanical engineering [14], and other subfields can be essential. The keyword and concept of sustainability can primarily explain the relationship, but this does not exclude other related areas.

The appropriate drainage of the railway permanent way is essential, which needs a well-formed subgrade crown and clean ballast. A supplementary layer is highly recommended to increase the structure's lifetime, which ensures drainage and can increase the geometrical stability of the railway track and the load-bearing capacity [15].

The authors made several tests with the geosynthetic cementitious composite material (GCCM) – type Concrete Canvas (CC) – to find out its behavior in the layer structure of the railway permanent way. Many case studies show the technology's widespread uses [16]. The earlier mentioned two essential functions can prove that it could be a useable technology in railways.

First of all, the CC is basically a material to ensure adequate drainage. Thanks to this, many ditches have been paved with this technology in the previous years. Nowadays, in Hungary, many problems have occurred from poor drainage or the weak subsoil. The two problems often generate each other, and the problem can easily become more serious. As it is known, the geometrical deterioration of a railway track is an exponential process, so weak support will soon affect the elements of the superstructure in line with the deterioration process of the railways. Unfortunately, in Hungary, there are many railway lines whose alignments run on embankments full of poor-quality soil, which needs permanent solutions. The most cost-effective intervention can be if drainage is constructed correctly in these cases. In these cases, two side ditches are not enough; adequate drainage is highly needed from the plane of the substructure [17, 18].

On the other hand, this GCCM technology could also ensure increasing ballast stability. In [19], the authors showed that ballast under loading can be pressed into the CC material, which means that the bottom layer of ballast is cemented into the layer which increases the inner shear resistance, as well as the case when geogrids are used. From this aspect, one of the aims of this article is to compare the behaviors and technical effects of geogrids in railway track structures.

In previous years, many studies have shown that using geogrids in railway track structures has many advantages and that it is not difficult for large railway construction machines to install [20]. The rolled-up transport method makes it easy to install the material in the railway track structure, and this is another link with CC because the CC is also delivered in this way [16, 21].

Nowadays, in Hungary, thanks to the European Union's support [22], several railway lines were fully renewed, but they reached less than 20 % of the total railway network. The authors believe that the investigated technology could be an appropriate solution for short sections where substructure problems occurred; on the other hand, it could be an appropriate solution for track maintenance.

Statement of the problem. This research is concerned only with railway engineering and according to the authors' experiences, particularly with Hungarian relations. Although CC has been experimentally installed in the road structure by Hungarian Public Roads Ltd., that case is a unique and separate experiment [23].

As mentioned in the introduction, the authors would like to find a fast, cost-effective, and easily installed solution with this technology, which can ensure dewatering problems and increase the geometrical stability of the structure.

The financial sources for the secondary railway lines are minimal, even though many existing defects affect the track's operational speed. Most of these problems occur due to the weak subgrade or subbase, mainly when the substructure contains clay, organic material, or other water-sensitive soils. Water affects some of the soils very much; thanks to this, the soil volume can be highly increased, and after drying, it can be "collapsed". In these cases, the most crucial exercise is to close the plane of the subgrade (and the slope of the embankment, too) from the rainwater. As it is known, the capillary water could still exist, but in this case, the surface precipitation is in focus. From this aspect, a good solution can be to asphalt the plane of the subgrade [24], but it needs complex organization. This is why renewing a whole or longer section can be a good solution, not a shorter local failure. As the authors aim to find a new solution for reconstructing short sections and local defects, they do not discuss this issue.

CC can be compared to the best way to planar geosynthetics, such as geogrid and geotextile, which are still excellent, easy-to-install solutions under the railway ballast. In addition, the geosynthetics product family, next to geogrids and geotextiles, also includes geomembranes, which are used to drain water under the ballast to protect the subgrade. According to the authors' experiences, the latter is a less used solution nowadays. The most used types are the geogrids and geotextiles (together: geocomposites), but the impact of geogrids is now highlighted. Geogrids installed directly under the railway ballast can stabilize the geometry of the railway track significantly. That means it can increase the lifetime of the track, which is an essential aspect. The crushed stone particles are wedged into the geogrid opening and held together by the geogrid's ribs or bands, as seen in Fig. 1. It increases the inner shear resistance in the lower zone in the railway ballast [25].

The inner shear resistance was measured in [26] with different types of geogrids in the mentioned multi-layer shear box. The graph of the summarized results showed that, on average, 14–15 % more inner shear resistance was measured on the 30 cm plane; the bottom 10 cm was also significantly stabilized. These results are easily comparable with CC measurements due to the existing test box and the ease of reconstructing the measurement.

Returning to the primary problem, the most used geosynthetics, for example, geotextiles, can improve the drainage but cannot entirely avoid the rainwater from the subgrade and the

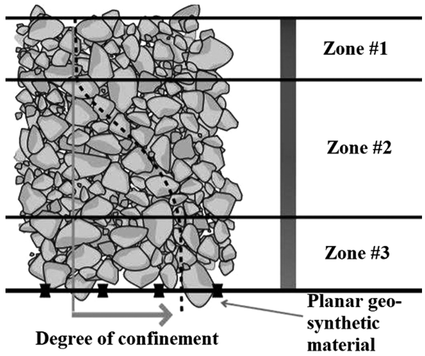

Fig. 1. The zones of the interlocking effect in a granular material on the basis of [21, 25]:

where Zone #1 is an intact zone; Zone #2 is a transition zone; Zone #3 is the affected zone

embankment. That is why geosynthetics cannot ensure complex solutions if the main problem is the lack of drainage.

To solve both problems, the geosynthetic cementitious composite mats, especially the CC layers, can be an alternative solution. The CC products contain three layers. A fibrous fabric is on the top, while the lower layer is waterproof PVC (polyvinyl-chloride). These two are connected by a 3D fiber matrix, while a unique cement mixture fills it [16]. According to official data scripts, the compressive strength reaches 80 % (but at least 50 MPa) after 24 hours of hydration, but the authors also did compression, 4-point bending, and puncture tests. Based on these previous investigations, the characterization and properties are 95–96 % after seven days [27].

In [19], the hypothesis was that the CC deforms under loading, and the ballast particles are penetrated into the CC. This hypothesis has been confirmed, so the interlocking effect was successfully observed. In Fig. 2, the theory is seen that the inner shear resistance in the bottom 10 cm was significantly increased. The increase was an average of 52 %. The ballast particles successfully wedged into the CC and cemented, so a large amount of crushed stone was hard to remove from the CC layer. In Fig. 2, the cemented particles were dark grey, while the surface with the shear resistance was marked with small red arrows.

In [19], it was proved that the CC layer is not punctured in this layer structure under this amount of loading (Fig. 3).

The objective of the article is to make a correct comparison between the CC tests with different preparations (loading time while bonding) and show the effectivity of the interlocking effect. In addition, another purpose is a comparison between the previous results from the different types of geogrids and a CC-reinforced layer structure. For this purpose, the needed basic parameters of the comparison are the loading of inner shear resistance, the tangent of the graph of the resistance, and the area calculated under the graphs. On the other hand, the wedged/cemented crushed stone particles ratio, the changing of surface flat, and the measurement of the load-bearing capacity are also important values to determine. The new shear tests had to be done in three planes, too. The authors aim to prove that the optional CC layer can solve complex problems

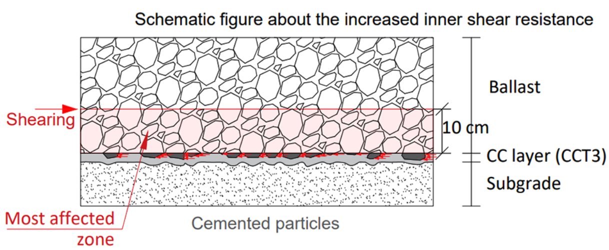

Fig. 2. Behavior of the CC under the railway ballast

Fig. 3. The bottom of the CC layer after the test. No puncture happened, and the lower PVC layer was not torn

like increasing the inner shear resistance more significantly while providing complete drainage.

Materials of the article. In this topic, investigations with the different types of geogrids were made in the laboratory of Széchenyi István University, Győr, in the 2010s. From these measurements, the multi-level shear box was given; thanks to this, the results were easy to use in this topic so that this research can be connected to geosynthetics-based inner shear resistance research. The related research was partly published in [26].

During the investigations, ballast crushed stone was andesite, with 31.5/50 mm "B type" grain sizes (i.e., the nominal minimum grain size was 31.5 mm; hence, the maximum is 50 mm) according to the MSZ EN standard [28]. This type of ballast had a breakage test in [29]. The sample was given by Colas Hungary Ltd., from the quarry of Szob, Hungary. There is a difference in this part of the tests; in the earlier investigations from the 2010s, it was 31.5/63 "E type".

In this research, the CC was purchased from Concrete Canvas Ltd. The authors decided to continue measuring in 7-day cycles. In [27], the measurements were executed with type CC13 (where 13 means the thickness of the material in the 'mm' unit); the new test was made with newer type CCT3. This is because the manufacturer has modified the structure and reduced the maximum thickness to 11 mm. The notable types are the CCT1, CCT2, and CCT3, with 5, 7 and 11 mm thicknesses. Nevertheless, the product range has expanded in recent years. Other types, like CCH, are available in 6 and 8 mm thicknesses (CCHT1 and CCHT2), respectively, with different structures and CCX, which also ensures a different layer structure and filler [16]. The authors decided and realized that the difference between the CC13 and the CCT3 is mainly the layer thickness; the experienced behavior will not be significantly modified. That means the results can be compared to each other.

In this measurement, the 3D laser scanner (GOM ATOS) was the same as before. GOM creates accurate 3D point clouds and measures with an accuracy of 0.01 mm [30] In [27], after the test, so-called flatness values were used to define the state of the CC layer's plane. In mechanical engineering, it is regulated by ISO 1101 [31]. With this procedure, the location of wedged stones can be detected with very high accuracy.

Methods. In [27], the authors stated that this measurement method is a valid methodology, so the tests' methodology was the same as before. The laboratory measurements were performed in a multi-level shear box, like in the first part.

The authors continue to reach the best load possibility for the CC. The well-compacted layer structure got a 100 kN vertical load to reach the nominal loading of 0.1 MPa (i.e., 10 N/cm^2), according to [15, 32].

So, while in the first part, the CC specimens were loaded beyond their (self) weight by 100 kN for a week, new tests in [19] show that minimal time of loadings is enough for the cementation of the ballast particles.

According to this, the authors planned a more realistic way to measure the effectiveness of the CC. At the new tests, the 100 kN initial loading was retained; only the load time was reduced from 7 days to 30 minutes. The previous preparation was adequate to show a measurement that can show valid results under a continuously loading railway track, while this change was made to model a situation when the CC was laid in under the structure, the superstructure was reconstructed, and then a railway working machine stays there for 30 minutes. After that, the hypothetical railway traffic is negligible. It is a quasi-realistic situation. After that, the CC got 7 kN/m^2 dead load from the ballast (~600 kg) and the loading steel plates (~100 kg).

The crushed stone layer was compacted in 20 cm thicknesses using an L-2/C plate vibrator. Its mass is 68 kg, and its power is 1.1 kW, with a nominal vibration rate of about 3,000 rotations/min. The size of the vibrating plate is 500 × 500 mm. The compaction was always carried out with the same number of passes to achieve the same amount of compaction work on the layers.

The measurements were executed in a multi-level shear box in October 2023 (Fig. 4). The layer structure was given thanks to the previous tests (Fig. 5). To make a correct comparison with geogrids, the authors tried to reach the same characteristics as in the previous tests from 2010–2012. From [27], the E_2 load-bearing capacity on the plane of the sandy gravel was 7.2 MPa, while the new measurements were made on a 5.8 MPa load-bearing surface. To be able to reach the necessary load-bearing capacity, only a sandy gravel layer was usable.

The thickness of the support layers was different because the authors could exchange the previous 40 cm XPS supported layer structure for two pieces of (2 cm thick each) under ballast mats (UBMs). It was also crucial because adequate elasticity could be reached; on the other hand, with only one layer of UBM, the load-bearing capacity was 18–19 MPa. Under the rubber mats, the floor (support) was a steel plate. It can be seen in Fig. 5.

Three shearing planes were determined. The total thickness of the ballast was 40 cm thick, so the 1st shearing was

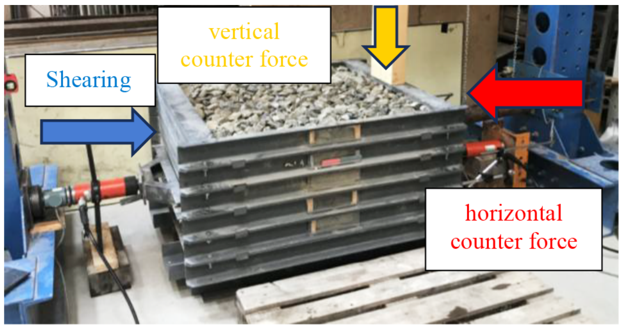

Fig. 4. The loading of the multi-level shear box

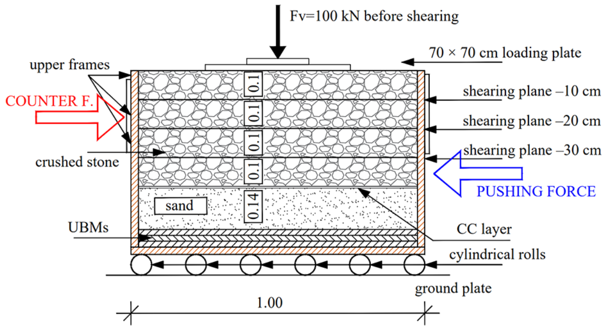

Fig. 5. The structure of the multi-level shear box

made – 10 cm, the 2^{nd} was made – 20 cm, and finally, the 3^{rd} was made – 30 cm from the top. The 3^{rd} plan is the most affected part. On – 40 cm, the measure was not made because the CC was laid on this plane; on the other hand, the CC could be broken from past experiences thanks to the cemented particles.

First, an initial measurement was performed without the CC layer to compare the results from the 2010–2012 test. After the evaluation, the results were close, so the authors found the study suitable for comparison with previous studies.

3D scanning at the initial state was not made; the previous study was well usable to compare. Thanks to the shear box's frame and the unchanged base layer in the flatness, significant differences could not happen.

In hydration, the author followed the methods from [27], watering directly the CC plane and watering after compacting the 20 cm ballast layer.

The tests were made after seven days of bonding for the best comparison. Then, the measurements were made on three planes to get the necessary data to see the amount of interlocking effect. To collect proper data, the frame had to be supported vertically to avoid the vertical movement of the frame due to the evolved torque.

After the measurement, the ballast particles were removed from the box as in the previous research [27]. It was vital to see and measure the weight of the cemented particles because this could be a spectacular comparison between the preparations. In this case, it must be mentioned that there were far fewer cases where a hammer had to be used to remove the ballast particles; most of it could be removed by hand.

The load-bearing capacity was measured according to the standards with a 300 mm steel plate and the necessary counterweight (loading) [33].

From [27], the state of the surface after the test was very rough. The authors also waited for fewer wedges stone particles into the CC due to the less vertical pre-loading. Finally, the differences between the initial and final surface at the new measurements were not as significant as in the previous measures where 100 kN vertical pre-loading was applied. The ballast particles are wedged into the CC material, but the amount of immovable stone particles was much less.

The contact surface was measured graphically, and after that, the surface was again measured by a GOM ATOS system, a 3D laser scanner, to measure the difference in the flatness. There were four tests, one without CC and three times with CC.

Results. The evaluation of the measurement was the same as in [27], but the final analysis was an extra part. The previous results were compared to each other and the geogrids' inner shear resistance results.

The measured inner shear resistance can be seen in Table 1; line 0 shows the average of the measurements of the layer structure without any reinforcement, while the second is the geogrid reinforced structure. The specimens are named 1.1–1.3 and 2.1–2.3, where the first number means the first or second type of measurement period, and 1–3 means the number of the sample.

The inner shear resistance is significantly increased compared to the measurements without CC. In Table 1, in the –10 and –20 cm zones, the resistance increased by 25–26 %, while in the lower plane, it increased on average by 57 % (that means 7 kN). The standard deviation only in the –20 cm zone was more significant; at the other layers, it was smaller.

In Table 2, a comparison can be seen between the previous and the new measurements. It must be mentioned that the high difference between the results is not only because of the "new" less loaded preparation. In the previous tests, only the bottom layer was sheared, while the new ones were in every zone. That means the upper ballast layers were moved while the compaction was much less at the time of the bottom zone loading. In Table 1 as described above, there is a significant difference between the previous and the new CC-reinforced measurements. On the other hand, in case 1, there is no data from the –10 and –20 cm planes, so case 1 is not included in Table 2.

The measurement with geocomposite reinforcement can be seen in Fig. 6. The typical inner shear resistance was between 13–15 kN, but it appears that a higher measurement has been made. The graph of the measurement results is shown in Fig. 6 and Table 2, which contains its evaluation. In Fig. 7, the authors, as in [27], visualized the inner shear resistance curves with the Concrete Canvas in the 0–55 mm horizontal displacement interval. The samples were reinforced by CC. Unfortunately, the resistance graph flattened as the shear resistance was removed, so the measurement was completed before the 55 mm horizontal displacement, but the result still gives a good picture. The graphs show that the maximum shear resistance is mostly higher in the case of CC reinforcement.

To make it possible to compare the CC results with the effect of the typical geogrids, the tangent of the graph in a horizontal 5–15 mm displacement was determined. In Table 3, the results were summarized in every shearing plane. In the last row of Table 3, the authors gave typical results with geocomposites from [26] to compare the data with the CC-reinforced results.

As it is seen, it is somewhat interesting that the average tangent of the geogrid reinforcement was nearly twice the other ones on the –10 and –20 cm plane, while on –30 cm, the tangent is nearly the same; there is no difference between the values.

Table 1

Results of the maximum inner shear resistance on the different shearing planes (Samples 2.1–2.3 are the cases "2.1–2.3 sample with CC")

No.	Average max. inner shear resistance, kN	Increase, %	Standard deviation	Relative standard dev., %
without reinforcement	12.17	–	1.856	15.3
with geocomposites/ geogrids	16.218	33.26	1.087	6.7
1.1–1.3 samples with CC	36.78	52.04	4.295	11.7
2.1–2.3 samples with CC	19.13	57.19	1.51	7.9

Table 2

Average results of maximal inner shear resistance on the different shearing planes [26]

No.	Maximal inner shear resistance in the different shearing planes, kN		
	–10 cm	–20 cm	–30 cm
average without reinforcement	3.78	8.24	12.17
with geocomposites/ geogrids	4.87	11.82	16.30
2.1–2.3 samples with CC	4.73	10.45	19.13
Standard deviation (CC)	0.67	4.50	1.51
Relative standard deviation (CC), %	14.2	43.1	7.9
Increasing compared to geogrid-reinforced case, %	–2.87	–11.59	17.36
Increasing compared to unreinforced case, %	25.13	26.82	57.19

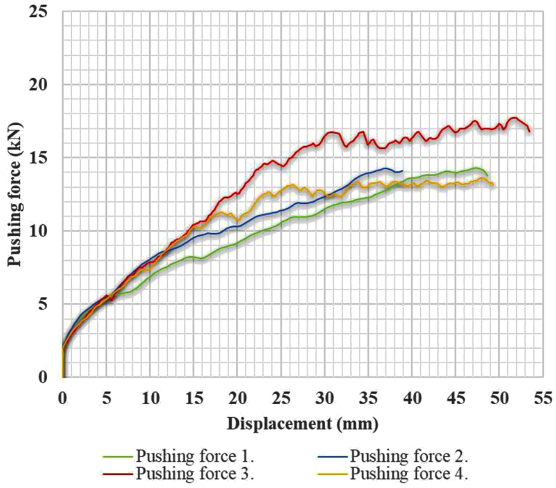

Fig. 6. Example of geogrid reinforcement: Typical compression-displacement diagram, with geocomposite reinforcement under a compacted crushed stone, shearing plane –30 cm [26]

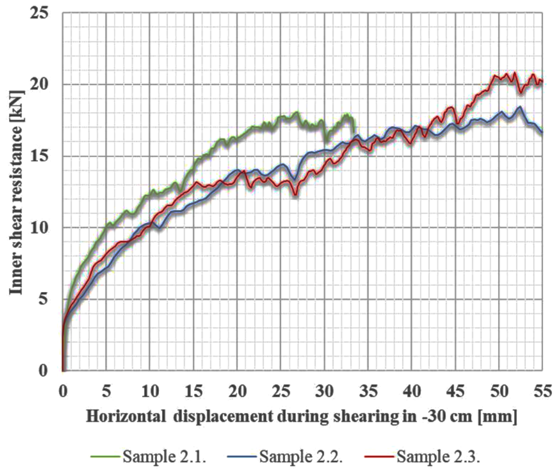

Fig. 7. Comparison of the inner shear resistance in a 0–55 mm horizontal displacement (shearing) interval at –30 cm plane

In the case of the longer pre-loaded samples, the average ratio between the tests and the geogrid reinforcement ones is 2.53. As concluded earlier, the measurement was significantly influenced by the longer pre-loading period and the reduced number of shear planes.

The following comparison is the calculation of the area under graphs by integration, as seen in Table 4. From previous experiences, the authors decided to investigate the 0–40 mm interval because of the enabled data. Unfortunately, during the test of sample "2.1", after reaching the maximal inner shear resistance, the test was stopped. Because of this, the mentioned sample cannot be evaluated from this aspect. It must be mentioned that [26] is dealing with this topic, and its research suggests that the most appropriate comparison method would be between 40–80 mm horizontal movement. This should be an essential consideration for future studies.

From the available data for evaluation, this approach showed the CC reinforced track structure to be stronger at –30 cm depth, while the upper layers on –10 and –20 cm are weaker.

The load-bearing capacity (E_2) was measured before and after the measurement. The initial load-bearing capacity was 5.96 MPa, the same as the previous measurement. It is crucial from the aspect of the comparisons. In [27], the average improved E_2 was 11.425 MPa, while in the second measurement series, the average of E_2 was 12.837 MPa. The average increasing was 115 %. From that, it can be stated that the effect of the tested CC13 and the CCT3 is nearly the same. The results of these tests are seen in Table 5. The measurements confirmed that further research in this area is also worthwhile.

After the load-bearing capacity measurements, the cemented particles were collected. As mentioned before, there were far fewer cases where a hammer had to be used to remove the ballast particles; most of it could be removed by hand, so the unmovable amount of the particle was decreased. The amount of cemented particles can be seen in Fig. 8. The authors got a big difference between the two types of measurements: while the more prolonged loading pressed the particles harder into the CC, the shorter time ensured that too, but with less effectiveness. In Table 6, the average cemented particles were 38.163 kg, while in the newer tests, this value was only 17.59 kg, representing a 54 % decrease. On the other hand, the previous tables and graphs showed that the inner shear resistance still increased by ~50 %, so the less cemented particles did not affect negatively.

In addition, it must be mentioned that the interlocking effect still happened from visualization.

As mentioned, the immovable stone particles were much less like the previous tests. It follows that fewer of the very conspicuous pressed areas were visible. The bedding areas were edited and re-evaluated by CAD software, as seen in Fig. 9. The calculated areas are shown in Table 7.

Table 3

The results of the tangent of the inner shear resistance in the 5–15 mm interval, comparison with the case of geogrid reinforced structure

No.	Tangent of the inner shear resistance in the 5–15 mm interval		
	–10 cm	–20 cm	–30 cm
with geocomposites/geogrids	0.300	0.436	0.424
1.1–1.3 samples with CC	–	–	1.070 (ratio: 2.53)
2.1–2.3 samples with CC	0.110	0.302	0.424
Standard deviation	0.048	0.128	0.065
Relative standard deviation, %	43.6	42.4	15.3
Ratio	0.37	0.69	1.00

Table 4

Calculating the area under the inner shear resistance graphs by integration in the 0–40 mm interval

No.	Area (kN·mm) under the inner shear resistance graphs on different shearing planes		
	–10 cm	–20 cm	–30 cm
with geocomposites/geogrids	278.718	544.546	285.487
2.1–2.3 samples with CC	187.057	272.152	442.345
Standard deviation	11.614	98.915	106.230
Relative standard deviation, %	0.062	0.363	0.240
Ratio	0.671	0.500	1.549

Table 5

Results of the measuring of load-bearing capacities

Average E_2, MPa		Standard deviation	Relative standard deviation	Average increasing
without reinforcement	2.1–2.3 samples with CC	MPa	%	%
5.96	12.837	0.413	0.032	115

Fig. 8. The amount of the wedged, unmovable ballast particles after the test

Table 6

The amount of cemented particles

Time of 100 kN vertical pre-loading	Average of cemented particles, kg	Standard deviation, kg	Relative standard deviation, %	Avr. w.p., %
7 days	39.64	2.565	0.065	6.853
30 min	17.59	1.363	0.077	3.03

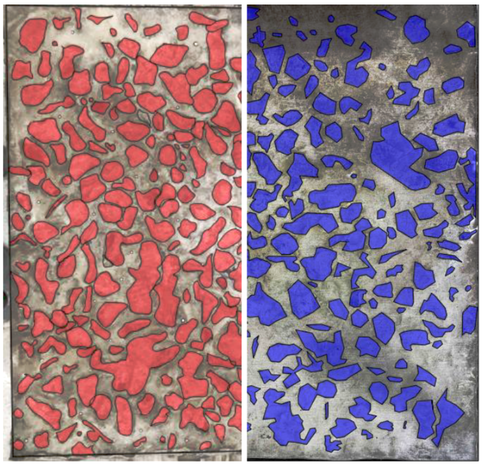

Fig. 9. The difference between the density of the locations of the wedged particles:

Left: 1 week pre-loading; Right: 30 minutes pre-loading

Table 7

Evaluation of the contact surface between the lowest "layer" of ballast and CC

Time of 100 kN vertical pre-loading	Full area	Contact area	Average	Standard dev.	Relative standard dev.
	m^2	m^2	%	%	%
7 days	1.01	0.49	48.48	0.854	0.018
30 min	0.99	0.37	37.37	0.980	0.026

As in [27], it must be mentioned that the graphical evaluation can contain some inaccuracy. According to the calculated area, the nominal loading on the CC was not the nominal 10 N/cm^2 loading from [15, 32]; in the newer tests on the cemented particles, it was 27.03 N/cm^2 instead. Of course, this is a theoretical approach, not an exact one.

After the tests, the deformations of the CC layers were analyzed by the GOM ATOS system. The final status after the investigation is shown in Fig. 10. As mentioned, a so-called flatness value can be measured from this test. The flatness value is used in mechanical engineering and regulated by ISO 1101 [31]. The average of the flatness values can be seen in Table 8.

It is seen that the samples with less vertical pre-loading had more minor flatness, too. On the other hand, compared to the sample before hydration, the flatness is still nearly double. Comparing Tables 6, 7 and 8, correlations were observed in the measured data. From them, it can be said that the lower inner shear resistance was not only due to fewer shearing planes but also due to the significant influence of less vertical pre-loading. The standard deviation was relatively smaller compared to experienced CC tests, so the accuracy of the measurements was appropriate.

As can be seen in Fig. 10, not the whole area was measured. This is due to the edges of the sample being elevated, reducing the accuracy significantly. This was observed, and the main problem was that the cement material "flowed" out from the layer structure during the preparation. However, theoretically, the loading was the same on the 1 × 1 m^2 area according to Fig. 10; the loading was probably more considerable in the interior parts.

Conclusions. This research was a second step to prove that the GCCM type Concrete Canvas (CC) can fulfill (or supplement) the geogrids, geotextiles, and geomembranes functions. In the first research, 100 kN vertical pre-loading was given to the sample, which caused the stone particles to be pressed and wedged into the CC layer, creating the so-called interlocking effect. In this second step, the measurement was made with less time of vertical pre-loading, which caused less cemented particles by 56 %. Besides the reduction, the strengthening effect has not changed. Although the inner shear resistance values decreased due to the more shearing planes and less loading time, the shear resistance increased by 52–57 % in proportion.

The results were compared to those of similar measurement with geosynthetic reinforcement and 31.5/50 mm "B

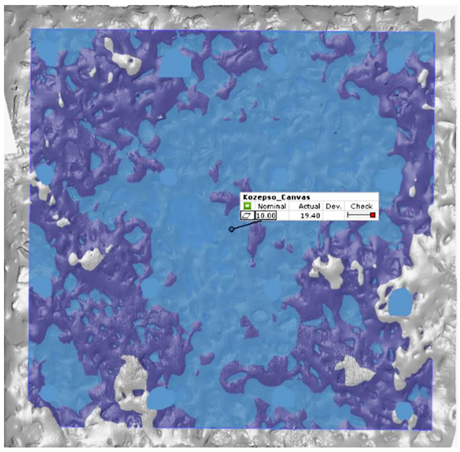

Fig. 10. Flatness evaluation of the 3D laser scanning

Table 8

Evaluation of the 3D laser scanning according to [30]

Specimen/Nr.	Hydration	Average of flatness	Stand. dev.	Relative stand. dev., %
before hydration	0 day	12.68	–	–
1.1–1.3 average with CC	7 days	28.63	5.799	20.3
2.1–2.3 average with CC	7 days	21.08	1.598	7.6

type" grain-sized railway ballast in the next step. It is seen that the inner shear resistance graphs are very similar, but from the tests, the resistance in the CC-reinforced structure was larger by 24 %. On the other hand, on the –10 and –20 cm plane, the tangent was higher in the geosynthetic reinforced structure, while on –30 cm, the tangent is nearly the same; there is no difference between the values. Finally, the areas under graphs were calculated by integration in the 0–40 mm horizontal interval. The results showed the same on the upper two shearing planes, they are much lower, but on –30 cm, the area was larger (with a high standard deviation).

From the analysis of the inner shear resistance results, the tested CC layers' surface, and the amount of wedged ballast particles, the authors found that although the inner shear resistance increases with the application of the CC layer, it continuously increases in proportion if the vertical pre-loading is also increased. Knowing the terms and conditions of the track closure, we can rule that the installed layer should be loaded after the ready-constructed superstructure as long as possible if the application could be available in the future.

To summarize the results, the Concrete Canvas provides adequate stabilization in the railway ballast.

References.

1. Gáspár, L., Horvát, F., & Lublóy, L. (2011). *Lifetime of transport infrastructure facilities*. Győr: Universitas-Győr Nonprofit Kft.

2. Kurhan, M.B., Kurhan, D.M., Husak, M.A., & Hmelevska, N. (2022). Increasing the efficiency of the railway operation in the specialization of directions for freight and passenger transportation. *Acta Polytechnica Hungarica*, *19*(3), 231-244. https://doi.org/10.12700/APH.19.3.2022.3.18.

3. Taran, I., & Litvin, V. (2018). Determination of rational parameters for urban bus route with combined operating mode. *Transport Problems*, *13*(4), 157-171. https://doi.org/10.20858/tp.2018.13.4.14.

4. Saukenova, I., Oliskevych, M., Taran, I., Toktamyssova, A., Aliakbarkyzy, D., & Pelo, R. (2022). Optimization of schedules for early garbage collection and disposal in the megapolis. *Eastern-European Journal of Enterprise Technologies*, *1*(3-115), 13-23. https://doi.org/10.15587/1729-4061.2022.251082.

5. Taran, I., & Bondarenko, A. (2017). Conceptual approach to select parameters of hydrostatic and mechanical transmissions for wheel tractors designed for agricultural operations. *Archives of transport*, *41*(1), 89-100. https://doi.org/10.5604/01.3001.0009.7389.

6. Czinder, B., Vásárhelyi, B., & Török, Á. (2021). Long-term abrasion of rocks assessed by micro-Deval tests and estimation of the abrasion process of rock types based on strength parameters. *Engineering Geology, 282*, 105996. https://doi.org/10.1016/j.enggeo.2021.105996.

7. Shehu, S.A., Yusuf, K.O., Zabidi, H., Jimoh, O.A., & Hashim, M.H.M. (2023). Blasting efficiency in granite aggregate quarry based on the combined effects of fragmentation and weighted environmental hazards. *Mining of Mineral Deposits, 17*(1), 120-128. https://doi.org/10.33271/mining17.01.120.

8. Haddad, J., Alfaqs, F., Al-quraan, T., & Ikhries, I.I. (2023). Investigation of vibrating jaw crusher experimental variables. *Mining of Mineral Deposits, 17*(3), 49-55. https://doi.org/10.33271/mining17.03.049.

9. Károlyfi, K. (2017). The effect of saturation degree of cement paste on fair-faced concrete surfaces. *Építöanyag*, (2), 55. https://doi.org/10.14382/epitoanyag-jsbcm.2017.10.

10. Kuchak, A.J.T., Marinkovic, D., & Zehn, M. (2020). Finite element model updating – Case study of a rail damper. *Structural Engineering and Mechanics, 73*(1), 27-35. https://doi.org/10.12989/sem.2020.73.1.027.

11. Kuchak, A.J.T., Marinkovic, D., & Zehn, M. (2021). Parametric Investigation of a Rail Damper Design Based on a Lab-Scaled Model. *Journal of Vibration Engineering and Technologies, 9*(1), 51-60. https://doi.org/10.1007/s42417-021-00341-7.

12. Szabó, V. A., & Dogossy, G. (2020). Investigation of flame retardant rPET foam. *Periodica Polytechnica Mechanical Engineering*, *64*(1), 81-87. https://doi.org/10.3311/PPme.14556.

13. Taran, I., & Klymenko, I. (2017). Analysis of hydrostatic mechanical transmission efficiency in the process of wheeled vehicle braking. *Transport Problems*, *12*(Special Edition), 45-56. https://doi.org/10.20858/tp.12.se.4.

14. Szabó, V.A., & Dogossy, G. (2017). Recycling of mineral water bottles with chemical foaming. *Acta Technica Jaurinensis*, *10*(2), 157-167. https://doi.org/10.14513/actatechjaur.v10.n2.446.

15. Fendrich, L., & Fengler, W. (2013). *Handbuch Eisenbahninfrastruktur*. Berlin: Springer Vieweg, Springer-Verlag.

16. *Concrete Canvas Ltd., Data Sheet* (2023, October 31). Retrieved from https://www.concretecanvas.com/uploads/CC-Data-Sheet-1.pdf.

17. Nagy, R. (2017). Description of rail track geometry deterioration process in Hungarian rail lines No. 1 and No. 140. *Pollack Periodica. 12*(3), 141-156. https://doi.org/10.1556/606.2017.12.3.13.

18. Nagy, R., & Horvát, F. (2021). Indirect determination of the measurement accuracy of the FMK-004 track geometry measuring car used on Hungarian rail network. *IOP Conference Series: Materials Science and Engineering – Computational Civil Engineering (CCE 2021)*, Iasi, Romania, 27–29 May, 2021, 012022. https://doi.org/10.1088/1757-899X/1141/1/012022.

19. Eller, B., Szalai, S., Movahedi, M.R., Fekete, I., Harrach, D., Baranyai, G., ..., & Fischer, S. (2023). Examination of Concrete Canvas under Quasi-Realistic Loading by Computed Tomography. *Infrastructures, 8*(2), 23. https://doi.org/10.3390/infrastructures8020023.

20. Das, B. M. (2016). Use of geogrid in the construction of railroads. *Innovative Infrastructure Solutions*, *1*, 1-12. https://doi.org/10.1007/s41062-016-0017-8.

21. *Tensar Brochure – Mechanical stabilisation of track ballast and subballast* (2023, October, 31). Retrieved from: https://www.scribd.com/document/537313092/Tensar-Railways.

22. *European Commission, Mobility and Transport* (2022, November 30). Retrieved from: https://transport.ec.europa.eu/transport-themes/infrastructure-and-investment_en.

23. Magyar Építéstechnika (2023, October 31). *Online journal on construction*. Retrieved from https://magyarepitestechnika.hu/index.php/epitoanyagok/innovacioval-az-utrehabilitaciokhoz/.

24. Khairallah, D., Blanc, J., Cottineau, L.M., Hornych, P., Piau, J.M., Pouget, S., ..., & Savin, F. (2019). Monitoring of railway structures of the high speed line BPL with bituminous and granular sublayers. *Construction and Building Materials*, *211*, 337-348. https://doi.org/10.1016/j.conbuildmat.2019.03.084.

25. Rakowski, Z. (2017). An Attempt of the Synthesis of Recent Knowledge About Mechanisms Involved in Stabilization Function of Geogrids in Infrastructure Constructions. *Procedia Engineering, 189*, 166-173. https://doi.org/10.1016/j.proeng.2017.05.027.

26. Fischer, S. (2023). Evaluation of inner shear resistance of layers from mineral granular materials. *Facta Universitas: Mechanical Engineering*. https://doi.org/10.22190/FUME230914041F.

27. Eller, B., Szalai, S., Sysyn, M., Harrach, D., Liu, J., & Fischer, S. (2023). Inner shear resistance increasing effect of Concrete Canvas in ballasted railway tracks. *Naukovyi Visnyk Natsionalnoho Hirnychoho Universytetu,* (2), 64-70. https://doi.org/10.33271/nvngu/2023-2/064.

28. Hungarian Standards Institute (2003). *MSZ EN 13450:2003. Aggregates for railway ballast*. Retrieved from https://ugyintezes.mszt.hu/webaruhaz/szabvany-adatok?standard=109857.

29. Fischer, S. (2017). Breakage Test of Railway Ballast Materials with New Laboratory Method. *Periodica Polytechnica Civil Engineering, 61*(4), 794-802. https://doi.org/10.3311/PPci.8549.

30. R-Design Studio, ATOS 5 (2023, October 31). *Metrology*. Retrieved from: https://r-design.hu/merorendszerek-szoftverek/atos/atos-5/.

31. International Organization for Standardization (2017). *ISO 1101:2017. Geometrical product specifications (GPS) — Geometrical tolerancing — Tolerances of form, orientation, location and run-out*. Retrieved from https://www.iso.org/obp/ui#iso:std:iso:1101:ed-4:v1:en.

32. Lichtberger, B. (2005). *Track compendium*. Hamburg: Eurailpress Tetzlaff-Hestra GmbH & Co. KG.

33. Hungarian Standards Institute (1989). *Bearing capacity test on pavement structures. Plate bearing test* (MSZ 2509-3:1989). Retrieved from https://ugyintezes.mszt.hu/webaruhaz/szabvany-adatok?standard=90404.

Переваги використання матеріалів CONCRETE CANVAS у будівництві залізничної колії

В. Еллер[1,2], *С. Салаї*[1], *М. Сисин*[3], *Д. Гаррах*[1], *Я. Лю*[4], *Ш. Фішер*[*1]

1 – Університет Сечені Іштвана, м. Д’єр, Угорщина
2 – Печський університет, м. Печ, Угорщина
3 – Інститут залізничних систем і громадського транспорту, ТУ Дрезден, м. Дрезден, Федеративна Республіка Німеччина
4 – Китайська залізниця Перша група Xinyun Engineering Co., Ltd, м. Сіань, Китайська Народна Республіка
* Автор-кореспондент e-mail: fischersz@sze.hu

Мета. Обгрунтування доцільності використання нових типів дренажних матеріалів типу Concrete Canvas (CC) під верхньою будовою колії залізниці.

Методика. Поставлені завдання вирішувалися комплексним методом дослідження, що включає аналіз й узагальнення літературних і патентних джерел, проведення аналітичних, експериментальних досліджень із використанням методів комп’ютерного й математичного моделювання. Випробування проводилися з використання CC шару та без нього в багаторівневому пристрої для зсувних випробувань. Після зсувного випробування зразки також перевірялися на несучу спроможність (E_2, згідно з Угорським стандартом) і на розрив частинок. Контактну поверхню між нижньою частиною баласту і CC виміряли за допомогою точного 3D-лазерного сканера (GOM ATOS) і візуалізували графічно за допомогою програмного забезпечення AutoCAD.

Результати. Експериментальне випробування вертикального навантаження під час з’єднання та аналіз результатів у порівнянні з результатами випробувань геокомпозитних/георешіткових конструкцій, внутрішнього опору зсуву та інших параметрів довели кращу несучу здатність конструкції з шаром CC. Виходячи з результатів, конструкція Concrete Canvas забезпечує вище зміцнення, ніж у середньому типи георешіток.

Наукова новизна. Уперше доведені переваги використання нових матеріалів Concrete Canvas у будові залізничній колії, що забезпечують більшу внутрішню стійкість до зсуву, ніж у середньому для георешіток.

Практична значимість. У майбутньому ці результати можуть забезпечити базові дані для використання конструкції Concrete Canvas у залізничній нижній та верхній будові колії.

Ключові слова: *залізниця, Concrete Canvas, баластна колія, внутрішня стійкость до зсуву, георешітка, GOM ATOS*

The manuscript was submitted 02.10.23.